sustainability

MDPI

Article

Effect of Common Ions in Agricultural Additives on the Retention of Cd, Cu, and Cr in Farmland Soils

Xu Zhou [1,2] and Hongbin Cao [1,2,*]

[1] Beijing Area Major Laboratory of Protection and Utilization of Traditional Chinese Medicine, Beijing Normal University, Beijing 100875, China; 202031051067@mail.bnu.edu.cn
[2] Faculty of Geographical Science, Beijing Normal University, Beijing 100875, China
* Correspondence: caohongbin@bnu.edu.cn

Abstract: The anions and cations in agricultural additives have crucial impacts on the retention of toxic heavy metals (HMs) in soil. However, the influence of these ions on the adsorption and desorption of Cd, Cr, and Cu in soil has not been clarified in previous studies. This study investigated the adsorption behavior of HMs, common anions, and dissolved organic matter (DOM) in alkaline soil from farmland under different experimental conditions. Nitrates, sulfates, and chlorides were used as HM sources to investigate the effects of different experimental anion environments on batch adsorption experiments and fluorescence quenching titration experiments. Batch sorption experiments showed that the sorption of Cd^{2+} was inhibited by the concomitant presence of Cr^{3+} and Cu^{2+}, and the presence of Cl^- and SO_4^{2-} inhibited the binding of HMs to the soil matrix compared to NO_3^-. The fluorescence quenching titration with HMs suggested that SO_4^{2-} significantly enhances the binding ability of Cr^{3+} to DOM in solution, which may be the reason SO_4^{2-} inhibited Cr^{3+} retention in soil. These results provide detailed insights into the interactions of HMs with DOM and anions, which is of great significance for the targeted application of pesticides and HMs' transport and removal in farmland soils.

Keywords: dissolved organic matter; EEM-PARAFAC; metal binding; coexisting anions; competitive sorption

check for updates

Citation: Zhou, X.; Cao, H. Effect of Common Ions in Agricultural Additives on the Retention of Cd, Cu, and Cr in Farmland Soils. *Sustainability* **2024**, *16*, 4870. https://doi.org/10.3390/su16114870

Academic Editor: Giancarlo Renella

Received: 24 February 2024
Revised: 28 May 2024
Accepted: 31 May 2024
Published: 6 June 2024

Copyright: © 2024 by the authors. Licensee MDPI, Basel, Switzerland. This article is an open access article distributed under the terms and conditions of the Creative Commons Attribution (CC BY) license (https://creativecommons.org/licenses/by/4.0/).

1. Introduction

Soil is an important nonrenewable resource, and problems associated with heavy metal (HM) pollution in soil are becoming increasingly severe due to industrial, agricultural, and other human activities [1]. HMs, such as Cu^{2+}, Cd^{2+}, and Cr^{3+}, in soil may come from wastewater irrigation, sewage sludge use, livestock manure applications, and atmospheric deposition [2,3]. The mobility and potential toxicity of HMs in soil depend on their retention and release within the soil matrix. Soil environment change can affect the ability of soil to retain and release HMs; these retention and release processes include precipitation and dissolution, ion exchange, and sorption/desorption reactions through inner-sphere and outer-sphere complexation [4]. The main physical and chemical factors governing these processes are pH and organic and inorganic colloids [5]. Competition exists among the different HMs in soil solutions, and HMs with high soil affinity affect those with lower affinity, thereby modifying their sorption ability [6–8]; the potential for the long-term release of metals should be considered in their risk assessment. Therefore, conducting competition experiments between two or more metals is important for understanding their relative affinity. However, there are still few studies on the sorption of three or more mixed cations onto agricultural soils at different concentrations.

Complex anions are often applied as part of fertilizers or pesticides and fungicides [4]. For example, the Bordeaux mixture can introduce a large amount of SO_4^{2-} and Cu^{2+} to the soil, nitrogen fertilizer contains a large amount of NO_3^-, and chlorine pesticides contain a large amount of Cl^-. These anions play an important role in the sorption of HMs to the

soil and thus change the environmental availability of HMs. Dahlin et al. [9] reported that adding Cl^- to soils with agricultural inputs strongly increased the concentration of Cd in crops by greatly mobilizing inherent soil Cd. Cl^- significantly increased the bioavailability and mobility of Cd in roots and promoted the transport of Cd from roots to shoots [10]. Kocik et al. [11] indicated that sulfates reduced surface charge repulsion, initiated ternary surface complexation, and enabled structural incorporation, which help enhance metal adsorption. However, metal coadsorption is reduced by solution complexation and surface site competition between metals and anions/ligands [5]. In general, changes in soil anions can affect the retention and release capacity of the HMs in the soil. Therefore, investigating the characteristics of HMs is highly important for promoting practices to prevent soil pollution in agriculture and maintain the safety of food products.

Dissolved organic matter (DOM) is a complex mixture of various organic molecules, including humic acid, fulvic acid, proteins, polysaccharides, and hydrophilic organic acids [12]. The active components in DOM, such as carboxyl and phenolic groups, can form complexes with HMs, leading to changes in HM migration, transformation, bioavailability, and toxicity in soils [13–16]. The types of organic components and HM cations present often play a crucial role in complex formation processes [17–20]. A series of advanced technologies, such as ultraviolet–visible spectroscopy (UV–Vis), Fourier infrared spectroscopy (FTIR), and fluorescence excitation-emission matrix (EEM) spectroscopy [21–23], were developed to characterize the complexation properties of DOM. In recent decades, parallel factor analysis (PARAFAC) has become a popular tool used to identify different independent groups of fluorescent components from overlapping fluorophores among the various compounds in EEM spectra [24–26]. This technique, combined with fluorescence quenching titration (the decrease in fluorescence due to an addition of metal), can provide more detailed information on complex binding characteristics [12,27]. Ryan et al. [28] reported a complexation model used to determine the binding parameters of fluorescent components derived from PARAFAC and HMs. The model can estimate the affinity of a single PARAFAC component with HMs by assuming a 1:1 ratio. For example, Zhang et al. [29] collected 13 representative forest soils in China and analyzed the characteristics of their DOM and its affinity for Cd using EEM+PARAFAC, and the impact of the interaction between HMs and DOM on the ecological toxicity and ecological risk of metals was emphasized. The inorganic anions and DOM in the soil can form complexes with HMs, leading to an increase in the concentration of HMs. This process can be beneficial for the dissolution and removal of HMs, however, there is limited research on the synergistic effects of these processes.

The incorporation of diverse agricultural inputs into arable land can contribute substantial amount of nutrients and trace elements to the soil, which can subsequently exert a significant influence on the geochemical behavior of HMs. Therefore, the objectives of this work were to (1) investigate the retention behavior of Cd^{2+}, Cr^{3+}, and Cu^{2+} via batch sorption experiments under both single-ion and multi-ion competitive sorption systems; (2) discuss the impact of SO_4^{2-}, NO_3^-, and Cl^- on the sorption of Cd^{2+}, Cr^{3+}, and Cu^{2+} onto soil; (3) and use EEM-PARAFAC to explore the HM binding characteristics of individual fluorescent components in DOM derived from an alkaline agricultural soil with representative HMs, including highly toxic Cd^{2+} and Cr^{3+}.

2. Methods

2.1. Soil Collection and Analyses

We selected a greenhouse vegetable planting area with fluvo-aquic soil in Tianjin, China, and collected natural soil samples (no industrial pollution). The soil samples were air-dried and screened through a 0.074 mm mesh sieve, and the soil pH was measured in 1:1.25 (v/v) soil–H_2O extracts with a pH meter (LpH-A, LABGIC, Beijing, China). Soil samples were digested using the tri-acid digestion method (Table S1), standard reference soil (GSS-1, Institute of Geophysical and Geochemical Exploration, Chinese Academy of Geological Science, Hebei, China) was used for quality control, and the contents of the HMs

(Cd^{2+}, Cr^{3+}, Cu^{2+}) were determined by ICP–OES (Optima 8000, PerkinElmer, Waltham, MA, USA). The dissolved carbon in the water was measured using a total organic carbon analyzer (TOC-LCPN Shimadzu, Kyoto, Japan). The soil particle size was determined by a laser particle size analyzer (Mastersize 3000, Malvern Panalytical, Malvern, UK). The detailed experimental method for the analysis of soil texture can be found in the Supplementary Materials. The basic properties of the soil are shown in Table 1. The soil used was completely mixed to maintain uniformity and minimize any variations in soil properties that could influence the sorption behavior of the HMs.

Table 1. Soil parameters for sorption experiments and DOM extraction.

Characteristics	pH (in Water)	Cd (mg kg^{-1})	Cu (mg kg^{-1})	Cr (mg kg^{-1})	TOC (Water Dissolved, mg kg^{-1})	Clay %	Silt %	Sand %
Soil sample	8.89	0.18 ± 0.03	20.23 ± 0.38	51.03 ± 0.83	80.2 ± 8.9	45.54	29.04	25.41

2.2. Batch Sorption Experiments

2.2.1. Single-Cation Sorption Experiment

To quantify the HM retention of the soils, a batch equilibration technique was used for a wide range of initial concentrations. $Cd(NO_3)_2{\cdot}4H_2O$, $Cr{\cdot}(NO_3)_3{\cdot}9H_2O$, and $Cu(NO_3)_2{\cdot}3H_2O$ were used to prepare single HM solutions at concentrations of 0.1, 0.2, 0.5, 1.0, 2, 3.5, 6, 8, and 10 mmol L^{-1}, respectively. Using 0.01 M $NaNO_3$ as the background electrolyte solution, 0.01 M HNO_3 and 0.01 M NaOH were used to adjust the solution pH to 5.0. Soil (1 g) was placed in a 50 mL Teflon centrifuge tube with 30 mL of a solution of Cd^{2+} (Cr^{3+} or Cu^{2+}) (30:1 m/v). A 3500 rpm shaker was used to agitate the solutions for 1 min to fully mix the solid and liquid, and then the solutions were placed in a constant shaker at 21.5 ± 1 °C and 180 rpm for 24 h to reach sorption equilibrium. The mixtures were centrifuged at 3500× g for 30 min and passed through a 0.45 µm filter membrane, and the supernatant was stored at 4 °C for measurement. The collected samples were analyzed using ICP–OES for Cd^{2+}, Cr^{3+}, and Cu^{2+} concentrations.

2.2.2. Competitive Cation Effects

To investigate the competitive adsorption between HM cations, a mixed solution of Cd^{2+}, Cr^{3+}, and Cu^{2+} was prepared. Nine initial concentrations of mixed HM solutions (0.1, 0.2, 0.5, 1.0, 2, 3, 5, 6, 8, 10 mmol L^{-1}) were prepared in a background solution of 0.01 M $NaNO_3$ (pH 5.0). Each solution contained the same concentration of Cd^{2+}, Cr^{3+}, and Cu^{2+}. For example, the first concentration setting contained 0.1 mmol L^{-1} Cd^{2+}, Cr^{3+}, and Cu^{2+}, while the second concentration setting contained 0.2 mmol L^{-1} Cd^{2+}, Cr^{3+}, and Cu^{2+}. The following settings were also the same. The experimental conditions, such as pH, temperature, and contact time, remained the same as in the single-cation sorption experiments.

2.2.3. Coexisting Anion Effects

To investigate the sorption behavior of the HM elements in different anion systems, the same mixed solutions of Cd^{2+}, Cr^{3+}, and Cu^{2+} were prepared as in Section 2.2.2, but using chloride or sulfate as the anionic component instead of nitrate. For instance, $2CdCl_2{\cdot}5H_2O$, $CrCl_3{\cdot}6H_2O$, and $CuCl_2{\cdot}2H_2O$ were used as chloride solutions, and 0.01 NaCl (M) was prepared as a background solution; $3CdSO_4{\cdot}8H_2O$, $Cr_2{\cdot}(SO_4)_3$, and $CuSO_4{\cdot}5H_2O$ were used as the sulfate solutions, and 0.01 M Na_2SO_4 was prepared as a background solution. The pH of all solutions was adjusted to 5.0 using related acids and NaOH; the other experimental conditions remained the same as in the competitive adsorption experiments.

2.3. Quenching Titration and Fluorescence Measurements

2.3.1. DOM Extraction

A total of 8 g of soil sample and 40 mL of ultrapure water were placed in a 50 mL centrifuge tube, and the tube was shaken (180 rpm) for 12 h at room temperature (22.5 °C),

centrifuged (3500 rpm) for 10 min, and then filtered through a 0.45 μm filter. The filtrates were kept in the dark at 4 °C. For all titrated DOM samples, the samples were diluted with ultrapure water to 10 mg L^{-1} to avoid inner filter effects [30].

2.3.2. Coexisting Anion Quenching Titration

A quenching titration was carried out by the addition of 0.01 mol L^{-1} Cd^{2+} (Cr^{3+} or Cu^{2+}) solution to 50 mL of diluted DOM samples in 100 mL brown vials. The final HM concentrations of the total solutions were in the range of 0~150 μmol L^{-1} (i.e., 0, 10, 20, 40, 60, 80, 100, 120, 150). To avoid dilution effects, the added volume of the HM solution was less than 1.5% of the total solution. The pH value was then adjusted to 4.0 by adding 0.1 M HCl or NaOH to establish a consistent pH before and after titration [31,32]. All solutions were shaken for 24 h at 25 °C to ensure complexation equilibrium. A quenching titration experiment was performed for Cd^{2+} (Cr^{3+} or Cu^{2+}) using chloride, nitrate, and sulfate sources to investigate the influence on the fluorescence intensity (FI) of different coexisting anions. The experimental conditions remained the same in different experimental groups.

Fluorescence EEMs were scanned over excitation (Ex) and emission (Em) wavelengths of 230–500 and 250–600 nm using a fluorescence spectrophotometer (F-7000, HITACHI, Tokyo, Japan). EEM spectra were collected by varying the scanning emission wavelength (Em) in 5 nm increments and the excitation wavelength (Ex) in 10 nm increments. The instrumental parameters were as follows: excitation and emission slits, 10 nm; scan speed, 2400 nm min^{-1}; and photomultiplier tube voltage, 700 V.

2.4. Data Analysis and Statistical Analysis

2.4.1. Sorption Experiment Analysis

The sorbed Cd^{2+}, Cr^{3+}, and Cu^{2+} were quantified by calculating the mass balance, and the sorption capacity of the natural soil Q (mmol kg^{-1}) can be described using Equation (1).

$$Q = \frac{(C_0 - C_1)V}{m} \quad (1)$$

where Q is the sorbed HM concentration, mmol kg^{-1}; C_0 and C_1 are the initial solution and supernatant concentrations after 24 h of sorption, respectively, mmol L^{-1}; V is the volume of the solution, L; and m is the mass of the soil, kg.

The sorption capacity of Cd^{2+} (Cr^{3+} or Cu^{2+}) in a single-cation system was compared with that in a competitive cation system (3 pairs, nitrate system); the sorption capacity of Cd^{2+} (Cr^{3+} or Cu^{2+}) in a competitive cation system was compared between different coexisting anions (9 pairs; nitrate, sulfate, and chloride systems). A paired *t*-test was used to examine the significance of the differences between each system.

Based on the batch sorption experiment results, the Cd^{2+}, Cr^{3+}, and Cu^{2+} sorption isotherms in the natural soil were analyzed using Freundlich models [33]. The sorption process was described based on the coefficient of determination (r^2) of the plots and the residual plots [34]. The general form of the sorption behavior can be described by the following equation:

$$S = K_f \cdot C^{\beta} \quad (2)$$

where S is the sorbed HM concentration, mmol kg^{-1}, which equals Q in this study; K_f and β are the soil–water distribution coefficients in the Freundlich exponent; and C is the HM concentration in the adsorption equilibrium solution, mmol L^{-1}.

2.4.2. PARAFAC Analysis and Complexation Modeling

PARAFAC analysis was performed using the free-download DOM Fluor toolbox in MATLAB (R2020b) to disintegrate the overlapping peaks of fluorophores into individual fluorescence substances according to a tutorial [35,36]. The maximum fluorescence intensity (F_{MAX}) could be obtained from the PARAFAC analysis to indicate the relative levels of individual components [37]. The complexation parameters between the PARAFAC-derived

components and metals were determined using the Ryan–Weber model [28], based on the assumption of a 1:1 complexation between the ligands and metals. The complexation parameters were obtained using the nonlinear fitting of Equation (3).

$$I = I_0 + (I_{ML} - I_0)\left(\frac{1}{2K_M C_L}\right)\left(1 + K_M C_L + K_M C_M - \sqrt{(1 + K_M C_L + K_M C_M)^2 - 4K_M^2 C_M C_L}\right) \quad (3)$$

where I and I_0 are the fluorescence intensities at the metal concentration C_M and at the beginning of titration (i.e., no metal addition), respectively; I_{ML} is the limiting value, below which the fluorescence intensity does not change upon the addition of a metal; K_M and C_L are the conditional stability constant and total ligand concentration, respectively, where higher K_M values correspond to stronger complexation stability.

In addition, the proportion of the fluorescence that corresponds to the binding fluorophores in the initial fluorescence (f) was determined using Equation (4).

$$f = \frac{(I_0 - I_{ML})}{I_0} \times 100 \quad (4)$$

A one-way ANOVA and multiple comparisons (Bonferroni) were conducted to assess the impact of different anions on the binding strength of Cd^{2+}, Cr^{3+}, or Cu^{2+} with the DOM solution. The quench rates of each DOM component when adding Cd^{2+}, Cr^{3+}, or Cu^{2+} to different anion systems were compared.

All experiments were repeated in triplicate, and data are expressed as the average value and standard deviation. The regression analysis and other statistical analyses were conducted using the Statistical Package SPSS 10.0. The PARAFAC was analyzed using Matlab R2020b (DOMfluor tool), the data visualization processing and Ryan–Weber model fitting were performed using Origin 2021.

3. Results and Discussion

3.1. Competitive Sorption Experiments

The physical, chemical, and biological reactions of HMs in solution with various components of soil determine the reaction behavior of HMs at the soil–liquid interface. The results of the single-cation sorption experiments and competitive sorption experiments are shown in Figure 1 (left). There is a significant difference in the adsorption performance between Cd, Cr, and Cu under the same conditions ($p < 0.001$). The slope coefficient values of the Cd^{2+}, Cr^{3+}, and Cu^{2+} sorbed in the single cation experiment are 10.27, 28.89, and 22.26, respectively, which are very different from the slope values for competitive sorption (5.39, 20.18, and 18.13). The results in Figure 1 suggest that Cd^{2+} was found to be the most competitively inhibited cation, and its single-cation sorption capacity showed a significant difference compared to the results of competitive adsorption experiments ($p = 0.003$); however, no significant difference was found for Cr^{3+} ($p = 0.054$) or Cu^{2+} ($p = 0.083$).

The metal sorption isotherms conformed to the Freundlich equation, as indicated by the high values for the correlation coefficient of determination (R^2) (Table 2). It is worth noting that, even at the highest concentration, none of the three HMs reached their maximum adsorption capacity, and the sorption capacity of Cd^{2+} was significantly lower than that of Cr^{3+} and Cu^{2+}. When multiple elements are in a soil system, competition among them for the same available sorption sites tends to suppress the strength and magnitude of element retention [38], and the ion radii of Cu^{2+} and Cr^{3+} are smaller than that of Cd^{2+}, which leads to their better affinity with soil.

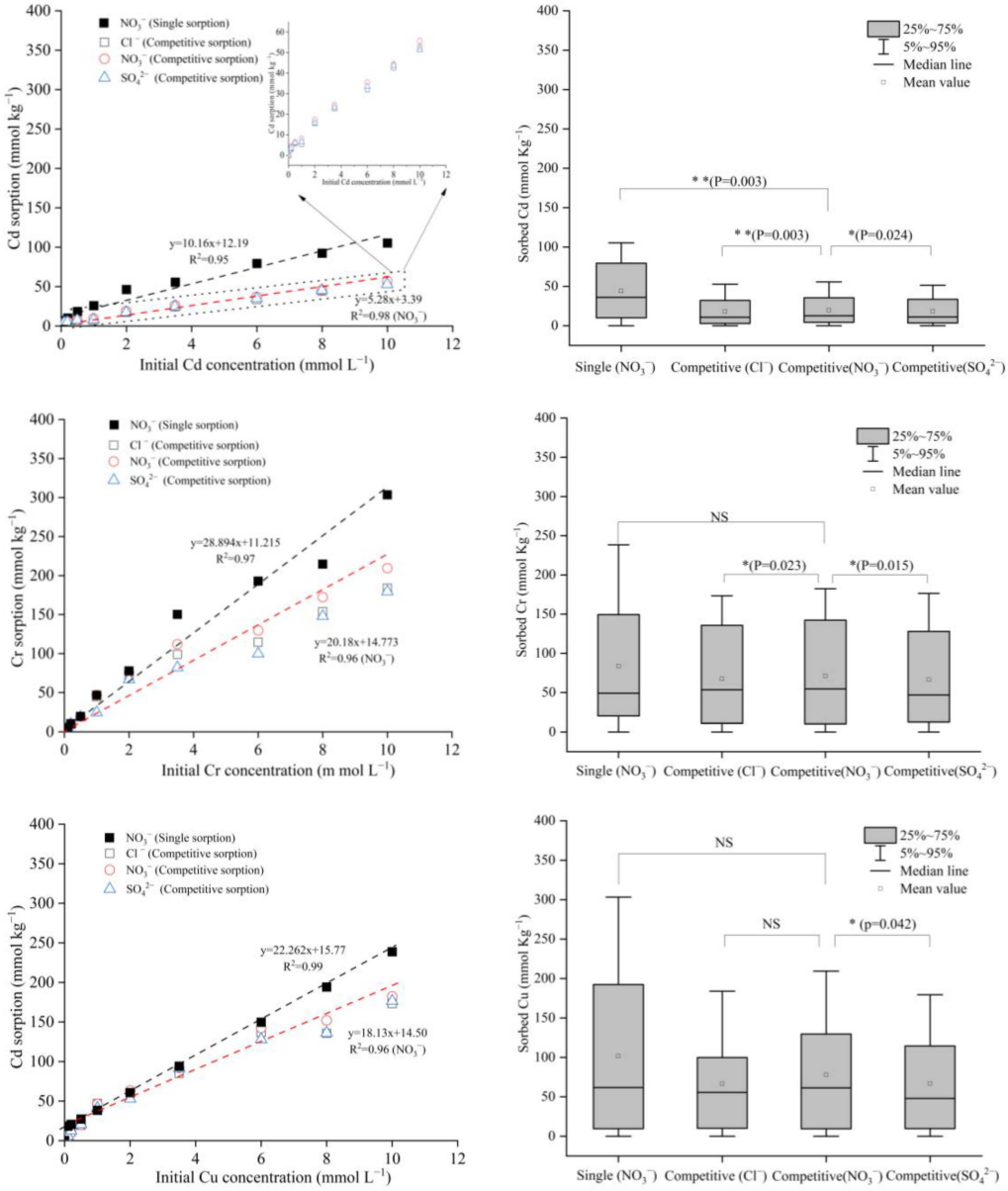

Figure 1. Comparison of sorbed metals as single and competitive cations in coexisting anion systems (**left**) and their paired-t significance test (**right**), **: $p < 0.01$; *: $p < 0.05$.

Table 2. The Freundlich sorption parameters of three HMs and their R-Square (R^2) values.

HMs	Coexisting Anions	Single Cations			Multiple Cations		
		K_f (mmol $^{1-\beta}$ L^{β} kg^{-1})	β	R^2	K_f (mmol $^{1-\beta}$ L^{β} kg^{-1})	β	R^2
Cd^{2+}	Cl^-	-	-	-	8.01	0.8	0.99
	NO_3^-	27.94	0.57	0.99	9.45	0.75	0.99
	SO_4^{2-}	-	-	-	8.81	0.76	0.99
Cr^{3+}	Cl^-	-	-	-	34.08	0.7	0.97
	NO_3^-	47.18	0.78	0.98	43.25	0.67	0.98
	SO_4^{2-}	-	-	-	36.8	0.68	0.98
Cu^{2+}	Cl^-	-	-	-	39.45	0.63	0.98
	NO_3^-	35.94	0.81	0.99	40.69	0.65	0.99
	SO_4^{2-}	-	-	-	39.69	0.66	0.99

In multi-competitive cation adsorption systems, the sorption preferences of soil toward HMs are different, and the main factors affecting sorption preferences are the hydrolysis constant, atomic weight, ionic radius, and, subsequently, the hydrated radius and Misono softness value of the HMs [39]. Mendes et al. [40] reported that, in a ternary HM system, soil's affinity for Cr was greater than that for Cu since soil exhibits a greater affinity for trivalent ions than for bivalent ions. The results of this study suggested that Cu^{2+} and Cr^{3+} mainly preempted the nonspecific sorption of Cd^{2+} in the soil through ion exchange, and the easily reversible adsorbed Cd^{2+} was released into the solution. Previous studies have indicated that most soils exhibit a greater affinity for Cu than for Cd because Cu^{2+} outcompetes Cd^{2+} for adsorption sites [41], and these results are similar to the findings in this study. The sorption preferences of fluvo-aquic soil for the three HMs were Cr > Cu > Cd, and the additional Cr and Cu in the soil increased the desorption of Cd, thereby increasing its mobility and environmental risk.

3.2. Coexisting Anion Sorption Experiments

HM salts of chlorine, nitrate, and sulfate were used as different HM sources. The results of the sorbed Cd^{2+}, Cr^{3+}, and Cu^{2+} levels and the paired *t*-test between different coexisting anion systems are shown in Figure 1(right). It is notable that, for almost all three HMs, NO_3^- significantly resulted in the retention of more HMs in the soil than Cl^- (Cd^{2+}: $p = 0.003$, Cr^{3+}: $p = 0.023$, Cu^{2+}: $p = 0.06$) and SO_4^{2-} (Cd^{2+}: $p = 0.024$, Cr^{3+}: $p = 0.015$, Cu^{2+}: $p = 0.042$). Cl^- led to the lowest sorption of Cd^{2+} in the soil across all concentration ranges, and SO_4^{2-} led to a significantly lower sorption of Cr^{3+} in the soil (Figure 1 and *p* value).

This phenomenon can be attributed, in part, to the formation of complexes between anions and HMs; Cl^- or SO_4^{2-} can form more complexes with HM cations compared to NO_3^-. It has been reported that Cd^{2+} and Cl^- can form complexes ($CdCl_n^{2-n}$), increasing the Cd^{2+} and TOC concentrations in soil solutions [42,43]. The organic matter dissolved in the solution will complex with HMs, affecting the sorption of HMs in the soil [20,44]. These findings suggest that anions, HM cations, and DOM may interact with each other, forming complexes when in solution. Nevertheless, our subsequent experiments demonstrated that the involvement of DOM in Cd^{2+} and Cl^- complexation is minimal. However, the impact of the interaction of SO_4^{2-}, DOM, and Cr^{3+} on complexation formation was obvious, which subsequently influenced the adsorption of Cr in the soil (Section 3.4).

3.3. DOM Characterization Using EEM-PARAFAC

Figure 2 illustrates the fluorescence spectra of the DOM components. Four individual components were identified by a PARAFAC analysis from natural soil-derived DOM. The sum of squared residuals and split half validation of PARAFAC can be found in Figures S1 and S2. OpenFluor, an online spectral library of autofluorescence in organic compounds, provides us with a method to characterize naturally occurring organic matter [45]. Component 1 (Ex/Em maxima: <260(320)/450 nm) and component 3 (Ex/Em maxima: 240(310)/430 nm) are usually described as humic-like components of terrestrial origin [46–48], while component 2 (Ex/Em maxima: <280/330 nm) resembles free and bound protein-like components [49]. The fluorophore of C2 exhibited EEM peaks resembling those of tyrosine-like components [17]. Component 4 (Ex/Em maxima: 260(360)/490 nm) has been reported to be a reduced quinone-like component and has been identified in DOM from a wide variety of aquatic systems [35,50]. Component 4 has also been found in many DOM samples from plant biomass and animal manure [51].

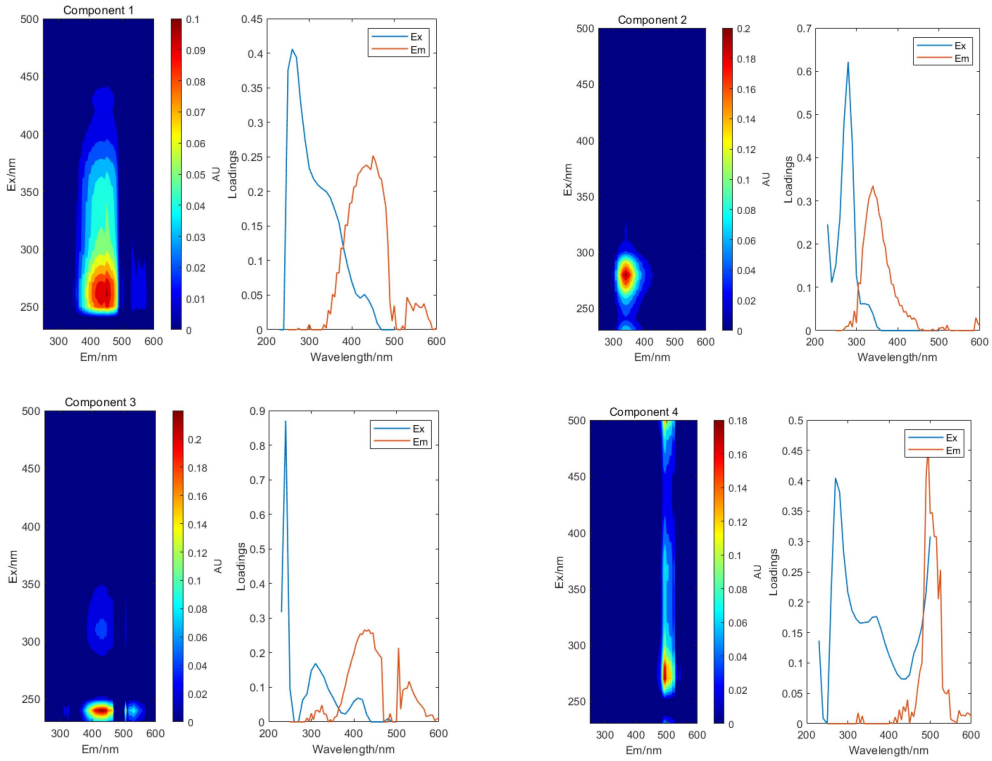

Figure 2. Four fluorescence components of soil-derived DOM identified using the EEM-PARAFAC model.

3.4. Behavior of Components with the Addition of Cu^{2+}, Cd^{2+}, and Cr^{3+}

The fluorescence intensity quenching results of the titrated DOM are presented in Figure 3. Marked differences among the four DOM components C1-C4 and between the three different metals were observed. The fluorescence intensity of C1-C4 decreased with the addition of Cu^{2+} and Cr^{3+}. The Ryan–Weber model parameters indicated that Cu^{2+} and Cr^{3+} exhibited a strong quenching effect on the four components (Table 3). Cd^{2+} only demonstrated a quenching of C2, and the fluorescence intensity of the C2 component decreased by 51% upon the addition of Cd^{2+}. Cd^{2+} showed little complexation with C1, C3, and C4, and our results were similar to those of other literature reports [29,52].

Table 3. Ryan–Weber model binding parameters of DOM with three HMs.

	Component	NO_3^-			SO_4^-			Cl^-		
		log_{KM}	f	R^2	log_{KM}	f	R^2	log_{KM}	f	R^2
Cd^{2+}	C1		FM			FM			FM	
	C2		FM			FM			FM	
	C3		FM			FM			FM	
	C4		FM			FM			FM	
Cr^{3+}	C1	5.20	59.67	0.98	5.34	85.63	0.98	5.56	58.57	0.96
	C2	4.89	70.97	0.94	6.24	85.79	0.99	4.93	81.30	0.97
	C3	5.22	60.27	0.96	5.26	78.20	0.98	5.37	68.51	0.98
	C4	5.08	57.84	0.98	5.50	86.68	0.98	5.72	72.02	0.98
Cu^{2+}	C1	4.75	55.41	0.97	4.7	44.68	0.94	4.66	50.26	0.95
	C2	6.00	82.15	0.99	5.01	77.80	0.95	5.82	85.4	0.99
	C3	4.74	57.49	0.97	4.73	54.37	0.95	4.93	53.15	0.94
	C4	4.91	71.39	0.99	4.77	63.34	0.97	4.86	66.09	0.97

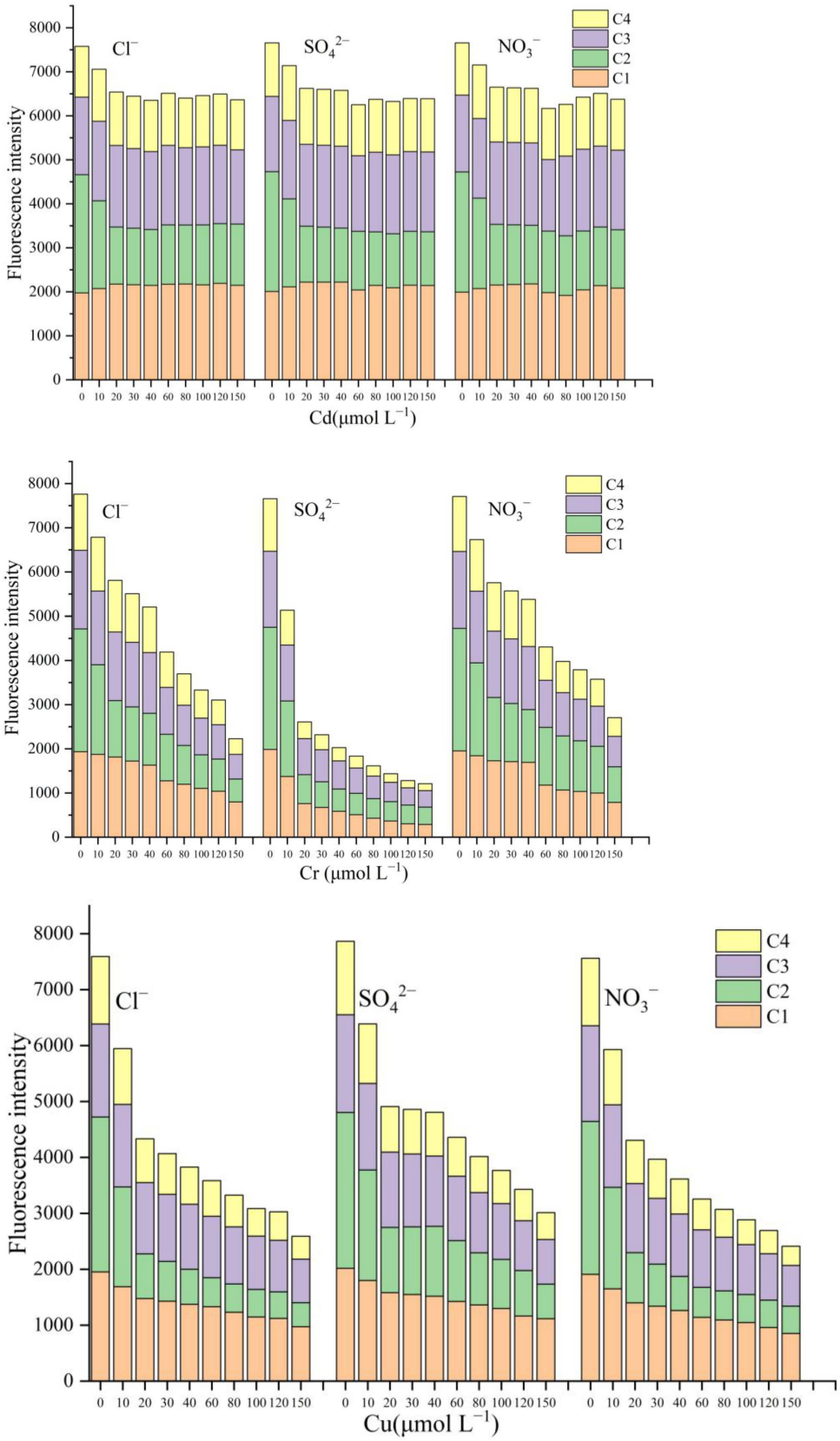

Figure 3. Variations in the F_{max} with the titration of three HMs.

The stability constants (log KM) calculated using the Ryan–Weber model for four PARAFAC-derived components and three HMs are listed in Table 3. C2 exhibits the highest affinity toward Cu^{2+}, and a similar effect was found in Cr^{3+} titrations; the log KM values

ranged from 4.89 to 5.22 and 4.74 to 6.00 for Cr^{3+} (NO_3^-) and Cu^{2+} (NO_3^-), respectively. The results show that the protein-like component (C2) shows greater stability than the humic-like acids (C1 and C3) (comprehensive judgment from log KM and f in Table 3), which validated the findings of other studies [17,53].

From the fluorescence quenching titrations with different coexisting anions, as seen in Figure 3 and Figure S3, it can be observed that the presence of SO_4^{2-} enhanced the degree of complexation between Cr^{3+} and each component (C1: $p = 0.004$, C2: $p = 0.61$, C3: $p = 0.085$, C4: 0.011 vs. Cl^-, C1: $p = 0.007$, C2: $p = 0.189$, C3: $p = 0.038$, C4: 0.008 vs. NO_3^-), with the total fluorescence intensity being 0.44 times (NO_3^-) and 0.54 times (Cl^-) what it was in the presence of the other two coexisting anions alternatively (150 µmol/L). Multiple comparisons, by ANOVA, of the quenching titrations (Table S2) indicated that all significant differences were found in the system with SO_4^{2-} as the anion. The fluorescence quenching titration results show that protein components have a better affinity for Cd^{2+}, Cr^{3+}, and Cu^{2+} than humic-like components. This is similar to previous research [31,54].

The coadsorption mechanisms present involve interfacial reactions between HM ions and anions, such as the formation of ternary surface complexes and surface precipitation, which can enhance the sorption of HM ions. However, solution complexation or competition for surface adsorption sites may reduce the soil's sorption capacity [5]. In this study, Cr^{3+}, which should be adsorbed on the soil surface by electrostatic attraction, existed in the solution by complexing with DOM components; in addition, SO_4^{2-} enhanced the binding of humic-like (C1) and reduced quinone-like (C4) component groups bonding with Cr^{3+}, leading to the significant promotion of complexation. Ali et al. [55] observed that the presence of nonsorbing Ca^{2+}-chelidamic acid complexes and phthalic acid led to a reduction in the sorption of Ca^{2+} on goethite in solution. Based on this observation, nonsorbing ternary surface complexes (DOM-Cr-sulfate) possibly formed, which could increase the Cr^{3+} concentration in the solution and diminish the retention of Cr^{3+} in the soil during coexisting anion sorption experiments. We did not observe similar phenomena for Cd^{2+} or Cu^{2+} (Figure 3 and Table S2), indicating the specificity of the interaction between Cr^{3+} and SO_4^{2+}. However, the chemical mechanism through which SO_4^{2+} enhances the complexation of Cr^{3+} with C1 and C4 in solution remains unclear. Further investigations should be conducted, including complexation experiments involving Cr^{3+}, DOM, and SO_4^{2+}, to clarify this phenomenon.

4. Conclusions

In-depth knowledge of the characteristics of HM retention in soil is essential for predicting the environmental behavior and evaluating the toxicology of HMs in agricultural soil and groundwater. Our study demonstrated that, in competitive cation systems, the sorption of HMs decreases, and Cd was the most inhibited by the coexistence of the other HMs. The concentration of HMs in the solution significantly increases when the coexisting anions in the soil–water system are Cl^- or SO_4^{2-}, especially for Cd^{2+} in the Cl^- system and Cr^{3+} in the SO_4^{2-} system. EEM-PARAFAC combined with batch sorption experiments can be used as an efficient approach to obtain a deeper understanding of the sorption affinity, binding capacity, and stability of HM binding with DOM in the environment. The DOM samples from typical greenhouse agricultural soil have different chemical compositions and metal-binding properties. EEM-PARAFAC showed a lower affinity of the soil DOM for Cd^{2+} than for Cu^{2+} and Cr^{3+}, even with protein-like components, which are the most active and show good complexation with other HMs. Humic-like components and reduced quinone-like components demonstrate little binding with Cd^{2+}. Furthermore, the influence of SO_4^{2-} on the percentage of DOM quenching and binding with Cr^{3+} indicated that coexisting anions can markedly change the DOM's metal-binding affinity, while the additional affinity between DOM and Cr^{3+} may lead to the low sorption of Cr^{3+} in soil. When high concentrations of HM ions coexist with sulfate ions and organic matter in the soil, their mobility should be further researched. DOM shows great potential as an additive to extract HMs from contaminated soil. This study provides experimental

data on the reduction of soil HM concentrations by common ions, and the results indicate that the efficiency of DOM additives in high-concentration Cr-contaminated soil may be improved by appropriately introducing sulfates.

Supplementary Materials: The following supporting information can be downloaded at https://www.mdpi.com/article/10.3390/su16114870/s1, Figure S1: The sum of squared residuals of PARAFAC; Figure S2: The split half validation curves of PARAFAC; Figure S3: Fluorescence excitation−emission matrix spectra of the NA soil−derived DOM during titration with Cd^{2+}, Cr^{3+}, and Cu^{2+} at concentrations from 20 to 150 μmol L^{-1} (0, 20, 40, 60, 120, 150). Cr + Cl^{-}: chloride salts are the source of Cr^{3+}, Cr + NO^{-}: nitrate salts are the source of Cr^{3+}, Cr + $SO_4{}^{2-}$: sulfate salts are the source of Cr^{3+}; Table S1: Pretreatment of soil and organic fertilizer samples; Table S2: Multiple comparisons after ANOVA of quenching titration.

Author Contributions: X.Z.: Methodology, Investigation, Formal analysis, Writing—original draft, Review and Editing, and Visualization. H.C.: Conceptualization, Methodology, Writing—original draft, Review and Editing, Supervision, and Project administration. All authors have read and agreed to the published version of the manuscript.

Funding: This study was supported by the National Key R&D Program of China (2018YFD0800404).

Institutional Review Board Statement: Not applicable.

Informed Consent Statement: The work described has not been published before; it is not under consideration for publication anywhere else; and written informed consent was obtained from individuals or the guardians of participants.

Data Availability Statement: The data that support the findings of this study are available from the corresponding author upon reasonable request. This work does not contain any research involving humans or animals.

Conflicts of Interest: The authors have no relevant financial or non-financial interests to disclose.

References

1. Dhaliwal, S.S.; Singh, J.; Taneja, P.K.; Mandal, A. Remediation techniques for removal of heavy metals from the soil contaminated through different sources: A review. *Env. Sci. Pollut R.* **2020**, *27*, 1319–1333. [CrossRef] [PubMed]
2. Peng, H.; Chen, Y.; Weng, L.; Ma, J.; Ma, Y.; Li, Y.; Islam, M.S. Comparisons of heavy metal input inventory in agricultural soils in North and South China: A review. *Sci. Total Env.* **2019**, *660*, 776–786. [CrossRef] [PubMed]
3. Shi, T.; Ma, J.; Wu, X.; Ju, T.; Lin, X.; Zhang, Y.; Li, X.; Gong, Y.; Hou, H.; Zhao, L.; et al. Inventories of heavy metal inputs and outputs to and from agricultural soils: A review. *Ecotox Env. Safe* **2018**, *164*, 118–124. [CrossRef] [PubMed]
4. Elbana, T.A.; Magdi Selim, H.; Akrami, N.; Newman, A.; Shaheen, S.M.; Rinklebe, J. Freundlich sorption parameters for cadmium, copper, nickel, lead, and zinc for different soils: Influence of kinetics. *Geoderma* **2018**, *324*, 80–88. [CrossRef]
5. Yan, Y.; Wan, B.; Mansor, M.; Wang, X.; Zhang, Q.; Kappler, A.; Feng, X. Co-sorption of metal ions and inorganic anions/organic ligands on environmental minerals: A review. *Sci. Total Env.* **2022**, *803*, 149918. [CrossRef] [PubMed]
6. Maity, S.K.; Tyagi, U.; Sirohi, S.; Pani, B.; Kumar, K.; Nikita; Kumar, G. Fabrication of biocompatible chitosan/graphene based nanocomposite for the competitive adsorption of heavy metal ions from wastewater in binary and ternary systems: Scale-up and upgradation studies. *J. Water Process Eng.* **2023**, *56*, 104555. [CrossRef]
7. Padilla, J.T.; Selim, H.M.; Gaston, L.A. Modeling the competitive sorption and transport of Ni(II) and Zn(II) in soils: Comparing two multicomponent approaches. *J. Contam. Hydrol.* **2023**, *252*, 104108. [CrossRef] [PubMed]
8. Chen, H.; Xiao, R.; Huang, D.; Deng, R.; Li, R.; Chen, Y.; Zhou, W. Three kinds of apatite adsorbents prepared by co-precipitation for Pb (II) and Cd (II) removal from wastewater: Performance, competitive effects and mechanisms. *J. Mol. Liq.* **2024**, *400*, 124478. [CrossRef]
9. Dahlin, A.S.; Eriksson, J.; Campbell, C.D.; Öborn, I. Soil amendment affects Cd uptake by wheat — are we underestimating the risks from chloride inputs? *Sci. Total Env.* **2016**, *554–555*, 349–357. [CrossRef]
10. Guo, J.; Ge, C.; Wang, G.; Zhou, D. Mechanisms of chloride to promote the uptake and accumulation of cadmium in rice (Oryza sativa L.). *Sci. Total Env.* **2024**, *926*, 172046. [CrossRef]
11. Kocik, E.M.; Kim, A.; Aiken, M.L.; Smith, L.; Kim, C.S. Sulfate enhances the adsorption and retention of Cu(II) and Zn(II) to dispersed and aggregated iron oxyhydroxide nanoparticles. *Appl. Geochem.* **2024**, *162*, 105929. [CrossRef]
12. Zhu, Y.; Jin, Y.; Liu, X.; Miao, T.; Guan, Q.; Yang, R.; Qu, J. Insight into interactions of heavy metals with livestock manure compost-derived dissolved organic matter using EEM-PARAFAC and 2D-FTIR-COS analyses. *J. Hazard Mater* **2021**, *420*, 126532. [CrossRef]

13. Fan, Q.; Sun, J.; Quan, G.; Yan, J.; Gao, J.; Zou, X.; Cui, L. Insights into the effects of long-term biochar loading on water-soluble organic matter in soil: Implications for the vertical co-migration of heavy metals. *Env. Int* **2020**, *136*, 105439. [CrossRef] [PubMed]
14. Kasmaei, L.S.A.F. Effect of organic matter on the release behavior and extractability of copper and cadmium in soil. *Commun. Soil Sci. Plan* **2012**, *43*, 2209–2217. [CrossRef]
15. Piccolo, A.; Spaccini, R.; De Martino, A.; Scognamiglio, F.; di Meo, V. Soil washing with solutions of humic substances from manure compost removes heavy metal contaminants as a function of humic molecular composition. *Chemosphere* **2019**, *225*, 150–156. [CrossRef] [PubMed]
16. Van Schaik, J.W.J.; Kleja, D.B.; Gustafsson, J.P. Acid–base and copper-binding properties of three organic matter fractions isolated from a forest floor soil solution. *Geochim. Cosmochim. Ac.* **2010**, *74*, 1391–1406. [CrossRef]
17. Chen, M.; Ding, S.; Li, C.; Tang, Y.; Fan, X.; Xu, H.; Tsang, D.C.W.; Zhang, C. High cadmium pollution from sediments in a eutrophic lake caused by dissolved organic matter complexation and reduction of manganese oxide. *Water Res.* **2021**, *190*, 116711. [CrossRef] [PubMed]
18. Li, H.; Yu, Y.; Chen, Y.; Li, Y.; Wang, M.; Wang, G. Biochar reduced soil extractable Cd but increased its accumulation in rice (Oryza sativa L.) cultivated on contaminated soils. *J. Soil Sediment* **2019**, *19*, 862–871. [CrossRef]
19. Luo, Y.; He, Y.; Zhou, D.; Pan, L.; Wu, Y. Organic amendment application affects the release behaviour, bioavailability, and speciation of heavy metals in zinc smelting slag: Insight into dissolved organic matter. *J. Hazard Mater* **2024**, *465*, 133105. [CrossRef]
20. Borggaard, O.K.; Holm, P.E.; Strobel, B.W. Potential of dissolved organic matter (DOM) to extract As, Cd, Co, Cr, Cu, Ni, Pb and Zn from polluted soils: A review. *Geoderma* **2019**, *343*, 235–246. [CrossRef]
21. Ly, Q.V.; Hur, J. Further insight into the roles of the chemical composition of dissolved organic matter (DOM) on ultrafiltration membranes as revealed by multiple advanced DOM characterization tools. *Chemosphere* **2018**, *201*, 168–177. [CrossRef] [PubMed]
22. Liu, D.; Gao, H.; Yu, H.; Song, Y. Applying EEM-PARAFAC combined with moving-window 2DCOS and structural equation modeling to characterize binding properties of Cu (II) with DOM from different sources in an urbanized river. *Water Res.* **2022**, *227*, 119317. [CrossRef] [PubMed]
23. Guo, X.; Peng, Y.; Li, N.; Tian, Y.; Dai, L.; Wu, Y.; Huang, Y. Effect of biochar-derived DOM on the interaction between Cu(II) and biochar prepared at different pyrolysis temperatures. *J. Hazard Mater* **2022**, *421*, 126739. [CrossRef] [PubMed]
24. Jin, Z.; Zhang, W.; Wang, X.; Liu, A.; Li, Z.; Bai, Y.; Wu, F. Leaching behaviors of dissolved organic matter from face masks revealed by fluorescence EEM combined with FRI and PARAFAC. *Water Res.* **2024**, *254*, 121399. [CrossRef]
25. Yang, L.; Chen, L.; Zhuang, W.; Zhu, Z. Unveiling changes in the complexation of dissolved organic matter with Pb(II) by photochemical and microbial degradation using fluorescence EEMs-PARAFAC. *Env. Pollut.* **2024**, *341*, 122982. [CrossRef]
26. Wells, M.J.M.; Funk, D.; Mullins, G.A.; Bell, K.Y. Application of a fluorescence EEM-PARAFAC model for direct and indirect potable water reuse monitoring: Multi-stage ozone–biofiltration without reverse osmosis at Gwinnett County, Georgia, USA. *Sci. Total Env.* **2023**, *886*, 163937. [CrossRef]
27. Liu, F.; Zhuang, W.; Yang, L. Comparing the Pb(II) binding with different fluorescent components of dissolved organic matter from typical sources. *Env. Sci. Pollut. R.* **2022**, *29*, 56676–56683. [CrossRef]
28. Ryan, D.K.; Weber, J.H. Fluorescence quenching titration for determination of complexing capacities and stability constants of fulvic acid. *Anal. Chem. (Wash.)* **1982**, *54*, 986–990. [CrossRef]
29. Zhang, X.; Li, Y.; Ye, J.; Chen, Z.; Ren, D.; Zhang, S. The spectral characteristics and cadmium complexation of soil dissolved organic matter in a wide range of forest lands. *Env. Pollut.* **2022**, *299*, 118834. [CrossRef]
30. Xing, J.; Xu, G.; Li, G. Analysis of the complexation behaviors of Cu(II) with DOM from sludge-based biochars and agricultural soil: Effect of pyrolysis temperature. *Chemosphere* **2020**, *250*, 126184. [CrossRef]
31. Wu, J.; Zhang, H.; Shao, L.; He, P. Fluorescent characteristics and metal binding properties of individual molecular weight fractions in municipal solid waste leachate. *Env. Pollut.* **2012**, *162*, 63–71. [CrossRef]
32. Wu, J.; Zhang, H.; He, P.; Shao, L. Insight into the heavy metal binding potential of dissolved organic matter in MSW leachate using EEM quenching combined with PARAFAC analysis. *Water Res.* **2011**, *45*, 1711–1719. [CrossRef]
33. Zhang, H.; Lu, K.; Zhang, J.; Ma, C.; Wang, Z.; Tian, X. Removal and Adsorption Mechanisms of Phosphorus, Cd and Pb from Wastewater Conferred by Landfill Leachate Sludge-Derived Biochar. *Sustainability* **2023**, *15*, 10045. [CrossRef]
34. Behroozi, A.; Arora, M.; Fletcher, T.D.; Western, A.W. Sorption and transport behavior of zinc in the soil; Implications for stormwater management. *Geoderma* **2020**, *367*, 114243. [CrossRef]
35. Stedmon, C.A.; Markager, S. Resolving the Variability in Dissolved Organic Matter Fluorescence in a Temperate Estuary and Its Catchment Using PARAFAC Analysis. *Limnol. Oceanogr.* **2005**, *50*, 686–697. [CrossRef]
36. Stedmon, C.A.; Bro, R. Characterizing dissolved organic matter fluorescence with parallel factor analysis: A tutorial. *Limnol. Oceanogr. Methods* **2008**, *6*, 572–579. [CrossRef]
37. Yang, L.; Han, D.H.; Lee, B.; Hur, J. Characterizing treated wastewaters of different industries using clustered fluorescence EEM–PARAFAC and FT-IR spectroscopy: Implications for downstream impact and source identification. *Chemosphere* **2015**, *127*, 222–228. [CrossRef] [PubMed]
38. Padilla, J.T.; Selim, H.M. Modeling the kinetics of competitive sorption and desorption of Zn(II), Ni(II), and Pb(II) in an acidic soil: Stirred-flow experiments. *Soil Sci. Soc. Am. J.* **2021**, *85*, 560–573. [CrossRef]

39. Shaheen, S.M.; Tsadilas, C.D.; Rinklebe, J. A review of the distribution coefficients of trace elements in soils: Influence of sorption system, element characteristics, and soil colloidal properties. *Adv. Colloid. Interfac.* **2013**, *201–202*, 43–56. [CrossRef]
40. Mendes, L.A.; Bucater, L.F.P.; Landgraf, M.D.; Rezende, M.O.O. Role of Organic Matter in the Adsorption/Desorption of Cr, Cu and Pb in Competitive Systems in Two Different Soils. *Open Access Libr. J.* **2014**, *1*, e1022. [CrossRef]
41. Cerqueira, B.; Covelo, E.F.; Andrade, L.; Vega, F.A. The influence of soil properties on the individual and competitive sorption and desorption of Cu and Cd. *Geoderma* **2011**, *162*, 20–26. [CrossRef]
42. López-Chuken, U.J.; Young, S.D. Modelling sulphate-enhanced cadmium uptake by Zea mays from nutrient solution under conditions of constant free Cd2+ ion activity. *J. Environ. Sci. (China)* **2010**, *22*, 1080–1085. [CrossRef]
43. Li, H.; Li, Z.; Khaliq, M.A.; Xie, T.; Chen, Y.; Wang, G. Chlorine weaken the immobilization of Cd in soil-rice systems by biochar. *Chemosphere* **2019**, *235*, 1172–1179. [CrossRef] [PubMed]
44. Jiang, S.; Dai, G.; Liu, Z.; He, T.; Zhong, J.; Ma, Y.; Shu, Y. Field-scale fluorescence fingerprints of biochar-derived dissolved organic matter (DOM) provide an effective way to trace biochar migration and the downward co-migration of Pb, Cu and As in soil. *Chemosphere* **2022**, *301*, 134738. [CrossRef] [PubMed]
45. Murphy, K.R.; Stedmon, C.A.; Wenig, P.; Bro, R. OpenFluor– an online spectral library of auto-fluorescence by organic compounds in the environment. *Anal Methods-Uk* **2014**, *6*, 658–661. [CrossRef]
46. Amaral, V.; Romera-Castillo, C.; Forja, J. Submarine mud volcanoes as a source of chromophoric dissolved organic matter to the deep waters of the Gulf of Cádiz. *Sci. Rep.* **2021**, *11*, 3200. [CrossRef] [PubMed]
47. Chen, M.; Park, M.; Kim, J.; Shinn, Y.J.; Lee, Y.K.; Hur, J. Exploring pore water biogeochemical characteristics as environmental monitoring proxies for a CO_2 storage project in Pohang Basin, South Korea. *Mar. Pollut. Bull.* **2018**, *137*, 331–338. [CrossRef] [PubMed]
48. Chen, M.; Kim, S.; Jung, H.; Hyun, J.; Choi, J.H.; Lee, H.; Huh, I.; Hur, J. Dynamics of dissolved organic matter in riverine sediments affected by weir impoundments: Production, benthic flux, and environmental implications. *Water Res.* **2017**, *121*, 150–161. [CrossRef] [PubMed]
49. Chen, M.; Price, R.M.; Yamashita, Y.; Jaffé, R. Comparative study of dissolved organic matter from groundwater and surface water in the Florida coastal Everglades using multi-dimensional spectrofluorometry combined with multivariate statistics. *Appl. Geochem.* **2010**, *25*, 872–880. [CrossRef]
50. Ohno, T.; Bro, R. Dissolved Organic Matter Characterization Using Multiway Spectral. *Soil Sci Soc. Am. J.* **2006**, *70*, 2028–2037. [CrossRef]
51. Hunt, J.F.; Ohno, T. Characterization of Fresh and Decomposed Dissolved Organic Matter Using Excitation−Emission Matrix Fluorescence Spectroscopy and Multiway Analysis. *J. Agr. Food Chem.* **2007**, *55*, 2121–2128. [CrossRef] [PubMed]
52. Huang, M.; Li, Z.; Luo, N.; Yang, R.; Wen, J.; Huang, B.; Zeng, G. Application potential of biochar in environment: Insight from degradation of biochar-derived DOM and complexation of DOM with heavy metals. *Sci. Total Env.* **2019**, *646*, 220–228. [CrossRef] [PubMed]
53. Huang, M.; Li, Z.; Huang, B.; Luo, N.; Zhang, Q.; Zhai, X.; Zeng, G. Investigating binding characteristics of cadmium and copper to DOM derived from compost and rice straw using EEM−PARAFAC combined with two-dimensional FTIR correlation analyses. *J. Hazard Mater* **2018**, *344*, 539–548. [CrossRef] [PubMed]
54. Shou, W.; Kang, F.; Lu, J. Nature and Value of Freely Dissolved EPS Ecosystem Services: Insight into Molecular Coupling Mechanisms for Regulating Metal Toxicity. *Env. Sci. Technol.* **2018**, *52*, 457–466. [CrossRef]
55. Ali, M.A.; Dzombak, D.A. Effects of simple organic acids on sorption of Cu^{2+} and Ca^{2+} on goethite. *Geochim. Cosmochim. Ac.* **1996**, *60*, 291–304. [CrossRef]

Disclaimer/Publisher's Note: The statements, opinions and data contained in all publications are solely those of the individual author(s) and contributor(s) and not of MDPI and/or the editor(s). MDPI and/or the editor(s) disclaim responsibility for any injury to people or property resulting from any ideas, methods, instructions or products referred to in the content.